Available online at www.sciencedirect.com
ScienceDirect
Signal Processing 86 (2006) 3456–3465
SIGNAL PROCESSING
www.elsevier.com/locate/sigpro

Noise-enhanced nonlinear detector to improve signal detection in non-Gaussian noise

David Rousseau[a,*], G.V. Anand[b], François Chapeau-Blondeau[a]

[a]*Laboratoire d'Ingénierie des Systèmes Automatisés (LISA), Université d'Angers, 62 avenue Notre Dame du Lac, 49000 Angers, France*
[b]*Department of Electrical Communication Engineering, Indian Institute of Science, Bangalore 560012, India*

Received 1 September 2005; received in revised form 23 January 2006; accepted 8 March 2006
Available online 30 May 2006

Abstract

We compare the performance of two detection schemes in charge of detecting the presence of a signal buried in an additive noise. One of these is the correlation receiver (linear detector), which is optimal when the noise is Gaussian. The other detector is obtained by applying the same correlation receiver to the output of a nonlinear preprocessor formed by a summing parallel array of two-state quantizers. We show that the performance of the collective detection realized by the array can benefit from an injection of independent noises purposely added on each individual quantizer. We show that this nonlinear detector can achieve better performance compared to the linear detector for various situations of non-Gaussian noise. This occurs for both Bayesian and Neyman–Pearson detection strategies with periodic and aperiodic signals.

Keywords: Detection; Quantizer; Nonlinear arrays; Suprathreshold stochastic resonance

1. Introduction

In presence of non-Gaussian noise, optimal detectors (in the standard Bayesian or Neyman–Pearson sense) are often nonlinear. Techniques, based on Hilbert space formalism, like in [1], can be used to derive optimal detectors in non-Gaussian noise. Yet, since optimal nonlinearities are rarely standard devices, these optimal detectors can be difficult to implement or time consuming to compute. In a context where simple processes are required to maintain fast real-time processing, one can seek a tradeoff between simplicity and efficacy by designing some suboptimal detectors. These suboptimal detectors are expected to be almost as simple to compute as the linear detector used in Gaussian noise with performances that should at least overcome the performances of the linear detector and hopefully come as close as possible to the optimal detector performances when the noise is non-Gaussian. In this suboptimal detection context, a classical approach [2,3] is to implement a nonlinear scheme composed of a nonlinear preprocessor followed by the linear scheme that would be used in a Gaussian noise.

In this article, following the approach of [2,3], we study a specific nonlinear preprocessor. We propose to design a simple suboptimal detector in non-Gaussian noise with a parallel array of two-state

*Corresponding author. Tel.: +33 241226511; fax: +33 241226561.
E-mail address: david.rousseau@univ-angers.fr (D. Rousseau).

0165-1684/$ - see front matter © 2006 Elsevier B.V. All rights reserved.
doi:10.1016/j.sigpro.2006.03.008

quantizers. Classically, the design of the input–output characteristic of such arrays is done by optimizing the distribution of the threshold of the quantizers among the array [4–8]. Here, we propose another strategy to design the input–output characteristic of our parallel array of two-state quantizers. Instead of considering a distribution of threshold, a single threshold value is shared by all the two-state quantizers of the array. Then, some independent noises are purposely injected at the input of each two-state quantizer. These noises injected onto the two-state quantizers, induce more variability and a richer representation capability in the individual responses collected over the array. We give a theoretical analysis which allows one to determine the optimal amount of the quantizer noises, this with arbitrary choices concerning the probability densities of the input and quantizer noises, the shape of the signals to be detected, and the configuration and size of the array of quantizers.

This non-standard strategy to design suboptimal detectors based on two-state quantizers benefits from recent studies on the use of stochastic resonance and the constructive role of noise in nonlinear processes [9–14]. This paradoxical nonlinear phenomenon, has been intensively studied during the last two decades. Stochastic resonance has been reported with nonlinear systems under the form of isolated two-state quantizers [15,16]. In these circumstances, the mechanism of improvement, qualitatively, is that the noise assists small signals in overcoming the threshold of the two-state quantizer. Recently, another form of stochastic resonance was proposed in [9,10], with parallel arrays of two-state quantizers, under the name of suprathreshold stochastic resonance. This form in [9–14] applies to signals of arbitrary amplitude, which do not need to be small and subthreshold, whence the name. Different measures of performance have been studied to quantify the suprathreshold stochastic resonance: general information measures like the input–output Shannon mutual information [9], the input–output correlation coefficient [11], signal-to-noise ratios [11,13], in an estimation context with the Fisher information contained in the array output [12] or in a detection context with a probability of error [14].

The first occurrence of the suprathreshold stochastic resonance effect in a detection context has been reported in [14]. The nonlinear detector under study in [14] is a Bayesian optimal detector based on the data set obtained at the output of the same nonlinear array of two-state quantizers considered here. As stated in [14], this detector is highly time consuming to compute and was more given as a first proof of feasibility of the suprathreshold stochastic resonance effect in the context of detection. By contrast, the present study proposes a more practical use of the suprathreshold stochastic resonance effect since the nonlinear detector detailed here is almost as fast as a linear detector to compute.

2. Two detection procedures

We consider the classical problem of detecting the presence of a known deterministic signal $s(t)$ buried in an additive input noise $\xi(t)$. One is to decide whether the signal $s(t)$ is present in noise (hypothesis H_1) or not (hypothesis H_0):

$$\text{hypothesis } H_1: x(t) = s(t) + \xi(t), \tag{1}$$

$$\text{hypothesis } H_0: x(t) = \xi(t). \tag{2}$$

The observable signal $x(t) = s(t) + \xi(t)$ is uniformly sampled to provide N data points $x(t_j) = x(j\tau)$ with $j = 0, 1, \ldots, N-1$ and τ the sampling step. The noise samples $\xi(t_j) = \xi(j\tau)$ are assumed independent and identically distributed with cumulative distribution $F_\xi(u)$, probability density function (pdf) $f_\xi(u) = \mathrm{d}F_\xi/\mathrm{d}u$ and rms amplitude σ_ξ. We first consider a Bayesian detection strategy where the probabilities (P_0, $P_1 = 1 - P_0$) of both hypotheses (respectively, H_0, H_1) are known. We tackle this detection problem with two distinct procedures presented in Fig. 1 that we shall describe in detail in this section.

2.1. A linear detector

In the procedure of Fig. 1a, the decision between (hypothesis H_1) and (hypothesis H_0) is directly based on the linear signal–noise mixture, the observable data set $\mathbf{x} = (x(t_0), x(t_1), \ldots, x(t_N))$. The minimum probability of error detection procedure based on $\mathbf{x}$ leads to the maximum a posteriori probability (MAP) test

$$\frac{\Pr\{H_1|\mathbf{x}\}}{\Pr\{H_0|\mathbf{x}\}} \underset{H_0}{\overset{H_1}{\gtrless}} 1. \tag{3}$$

When the input noise $\xi(t)$ is Gaussian, the MAP test of Eq. (3) takes the form of the detection procedure described in Fig. 1a [2]: a correlation receiver which computes the statistic $T(\mathbf{x}) = \sum_{j=0}^{N-1} x(t_j)s(t_j)$ is

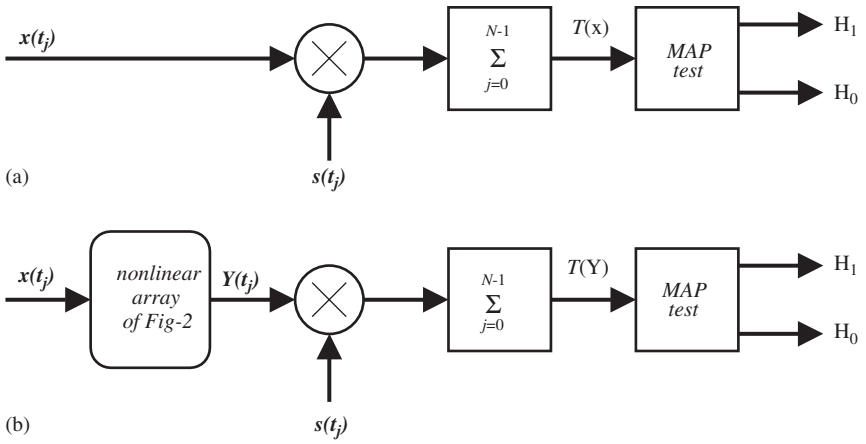

Fig. 1. Two detectors that we shall compare in terms of performance. The linear detector (a) is a standard procedure optimal for Gaussian noise. The nonlinear detector (b) is a new procedure keeping the same architecture of (a) with the introduction of a nonlinear preprocessor detailed in Fig. 2.

followed by the MAP test based on this statistic $T(\mathbf{x})$:

$$T(\mathbf{x}) \underset{\mathrm{H}_0}{\overset{\mathrm{H}_1}{\gtrless}} \frac{1}{2}\sum_{j=0}^{N-1} s(t_j)^2 + \sigma_\xi^2 \log(P_0/P_1) = x_T. \tag{4}$$

The performance of the detection procedure of Fig. 1a can be assessed by the overall probability of error minimized by Eq. (4) which is expressed as

$$P_{\mathrm{er}} = \frac{1}{2}\left[1 + P_1 \,\mathrm{erf}\left(\frac{x_T - m_1}{\sqrt{2}\,\sigma_1}\right) - P_0 \,\mathrm{erf}\left(\frac{x_T - m_0}{\sqrt{2}\,\sigma_0}\right)\right], \tag{5}$$

with $\mathrm{erf}(u) = \int_{-\infty}^{u} (1/\sqrt{2\pi}) \exp(-v^2/2)\,\mathrm{d}v$, means $m_0 = E[T(\mathbf{x})|\mathrm{H}_0]$, $m_1 = E[T(\mathbf{x})|\mathrm{H}_1]$ and variances $\sigma_0^2 = \mathrm{var}[T(\mathbf{x})|\mathrm{H}_0]$, $\sigma_1^2 = \mathrm{var}[T(\mathbf{x})|\mathrm{H}_1]$.[1] When the input noise $\xi(t)$ is non-Gaussian, the optimal detector minimizing the probability of error, in general, is more difficult to design and the MAP test of Eq. (3) does not lead to a simple test as simple as in Eq. (4). However, the detection procedure of Eq. (4) although suboptimal when the input noise is non- Gaussian is often chosen for its simplicity. By the central limit theorem, the statistic $T(\mathbf{x})$ is approximately Gaussian for large data set length N. Therefore, when the input noise $\xi(t)$ is non-Gaussian, the performance of the detector of Eq. (4) and Fig. 1a given in Eq. (5) remains valid.

[1]Note that, in this context of additive signal–noise mixture of Eqs. (1) and (2) $\sigma_0 = \sigma_1 = \sigma_\xi$, $m_0 = \sum_{j=0}^{N-1} s(t_j)E[\xi(t_j)]$ and $m_1 = \sum_{j=0}^{N-1} s(t_j)^2$.

2.2. A nonlinear detector

The detection procedure of Fig. 1b is similar to the procedure of Fig. 1a except that the data set $\mathbf{x}$ obtained from the linear signal–noise mixture $x(t) = s(t) + \xi(t)$ is not directly observable. The data set $\mathbf{x} = (x(t_1), \ldots, x(t_N))$ is first applied at the input of a nonlinear preprocessor which produces a vector $\mathbf{Y} = (Y(t_1), \ldots, Y(t_N))$ on which we shall base the decision between (hypothesis H_1) and (hypothesis H_0). The detection procedure of Fig. 1b is then composed of a correlation receiver which computes the statistic $T(\mathbf{Y}) = \sum_{j=0}^{N-1} Y(t_j)s(t_j)$ followed by the MAP test based on this statistic $T(\mathbf{Y})$,

$$\frac{\Pr\{\mathrm{H}_1|T(\mathbf{Y})\}}{\Pr\{\mathrm{H}_0|T(\mathbf{Y})\}} \underset{\mathrm{H}_0}{\overset{\mathrm{H}_1}{\gtrless}} 1. \tag{6}$$

The nonlinear preprocessor involved in the detection procedure of Fig. 1b is a parallel array of M identical two-state quantizers which has an architecture similar to the one also considered in [9,17,18]. In this array of Fig. 2, we choose to fix all the quantizer threshold θ_i to a common value $\theta_i = \theta$ for any i. Then, a noise $\eta_i(t)$, independent of $x(t)$, is added to $x(t)$ at each two-state quantizer i. Whereas the input noise $\xi(t)$ is considered as a noise imposed by the external environment, the quantizer noises $\eta_i(t)$ are considered as purposely added noises applied to influence the operation of the array. Accordingly, each quantizer i produces the output signal,

$$\begin{aligned} y_i(t_j) &= \mathrm{sign}[x(t_j) + \eta_i(t_j) - \theta_i] \\ &= \pm 1, \quad i = 1, 2, \ldots M. \end{aligned} \tag{7}$$

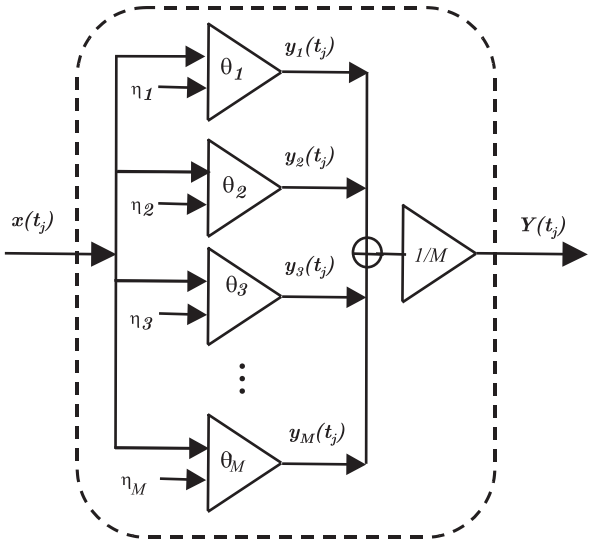

Fig. 2. Nonlinear array used as preprocessor in the detection scheme of Fig. 1b.

The M quantizer noises $\eta_i(t)$ are white, mutually independent and identically distributed with cumulative distribution function $F_\eta(u)$ and pdf $f_\eta(u) = \mathrm{d}F_\eta(u)/\mathrm{d}u$. The response $Y(t_j)$ of the array is obtained by averaging the outputs of all the quantizers as

$$Y(t_j) = \frac{1}{M}\sum_{i=1}^{M} y_i(t_j). \tag{8}$$

At the scale of the individual quantizer, the presence of the quantizer noises $\eta_i(t)$ can be interpreted as a source of variability which enable a richer representation capability when individual responses are collected over the array. Another complementary interpretation is possible with a collective point of view. Consider the array as a single device with input–output characteristic $g(.)$. Within this perspective, the quantizer noises $\eta_i(t)$ are modifying the input–output characteristic of the array $g(.)$. Naturally, the M quantizers noises $\eta_i(t)$ also bring fluctuations. But, for sufficiently large values of M these fluctuations will tend to zero. In these asymptotic conditions where M tends to infinity, the parallel array of noisy quantizers given in Eq. (8) becomes a deterministic equivalent device with input–output characteristic given by $g(x) = E[Y(t)|x]$. Therefore, the purposely added noises $\eta_i(t)$ can be seen as a mean to shape the input–output characteristic $g(.)$ of the array of comparators without having to change any physical parameter of the comparators.

In the following, we are going to compare the two detection procedures presented in Fig. 1 and show the specific interest of the nonlinear array of Fig. 2 for detection purposes. Owing to the presence, in Eq. (4), of the linear correlation receiver acting on the linear signal–noise mixture in the detection procedure of Fig. 1a, we decide to call linear detector this detection procedure. By comparison, the detection procedure of Fig. 1b, which involves the nonlinear preprocessor described in Fig. 2, will be called the nonlinear detector.

3. Assessing performances of the nonlinear detector

In this section, we give the expression of the performance (in terms of probability of error) of the nonlinear detector of Fig. 1b and Eq. (6). By Bayes' rule, the MAP test of Eq. (6) is equivalent to

$$\frac{\Pr\{T(\mathbf{Y})|\mathrm{H}_1\}}{\Pr\{T(\mathbf{Y})|\mathrm{H}_0\}} \underset{\mathrm{H}_0}{\overset{\mathrm{H}_1}{\gtrless}} \frac{P_0}{P_1}, \tag{9}$$

with the conditional probabilities $\Pr\{T(\mathbf{Y})|\mathrm{H}_1\}$ and $\Pr\{T(\mathbf{Y})|\mathrm{H}_0\}$ that we shall now address. The statistic $T(\mathbf{Y})$, defined through Eqs. (7) and (8) has mean

$$\begin{aligned} m_k &= E[T(\mathbf{Y})|\mathrm{H}_k] \\ &= \sum_{j=0}^{N-1} s(t_j) E[Y(t_j)|\mathrm{H}_k], \quad k \in \{0,1\}, \end{aligned} \tag{10}$$

with

$$E[Y(t_j)|\mathrm{H}_k] = \int_{-\infty}^{+\infty} E[Y(t_j)|x;\mathrm{H}_k] f_\xi(x - s(t_j))\,\mathrm{d}x, \tag{11}$$

and, since the quantizer noises $\eta_i(t)$ are i.i.d.,

$$E[Y(t_j)|x;\mathrm{H}_k] = E[y_i(t_j)|x;\mathrm{H}_k] = 1 - 2F_\eta(\theta - x). \tag{12}$$

Similarly, the variance of $T(\mathbf{Y})$ under hypothesis $k \in \{0,1\}$ can be expressed as

$$\begin{aligned} \sigma_k^2 &= \mathrm{var}[T(\mathbf{Y})|\mathrm{H}_k] \\ &= \sum_{j=0}^{N-1} s(t_j)^2 (E[Y^2(t_j)|\mathrm{H}_k] - E[Y(t_j)|\mathrm{H}_k]^2) \end{aligned} \tag{13}$$

with

$$\begin{aligned} &E[Y^2(t_j)|\mathrm{H}_k] \\ &\quad = \int_{-\infty}^{+\infty} E[Y^2(t_j)|x;\mathrm{H}_k] f_\xi(x - s(t_j))\,\mathrm{d}x \end{aligned} \tag{14}$$

and

$$E[Y^2(t_j)|x;\mathrm{H}_k] = \frac{1}{M}E[y_i^2(t_j)|x;\mathrm{H}_k] + \frac{M-1}{M}E^2[y_i(t_j)|x;\mathrm{H}_k] \quad (15)$$

and, because of Eq. (7), one has for any i

$$E[y_i^2(t_j)|x;\mathrm{H}_k] = 1. \quad (16)$$

When N is large, thanks to the central limit theorem, $T(\mathbf{Y})$ gets normally distributed. The conditional probabilities in Eq. (9) are then given by

$$\Pr\{T(\mathbf{Y})|\mathrm{H}_k\} = \frac{1}{\sigma_k\sqrt{2\pi}}\exp\left[-\frac{(T(\mathbf{Y})-m_k)^2}{2\sigma_k^2}\right], \quad (17)$$

and the loglikelihood-ratio test derived from Eq. (6) follows as

$$\log\left(\frac{\sigma_0 P_1}{\sigma_1 P_0}\right) + \frac{(T(\mathbf{Y})-m_0)^2}{2\sigma_0^2} - \frac{(T(\mathbf{Y})-m_1)^2}{2\sigma_1^2} \underset{\mathrm{H}_0}{\overset{\mathrm{H}_1}{\gtrless}} 0. \quad (18)$$

With the only condition of a large data set (i.e. when N is large[2]), the performance of the nonlinear detector of Fig. 1b can be calculated with the algorithm of Fig. 3. This algorithm has already been described in [19] for specific conditions (constant signal $s(t) \equiv s_0$ or s_1 and a statistic performed on a 1-bit representation of the input signal x). Although not highlighted in [19], the algorithm of Fig. 3 can, in fact, be applied generically to any situation of detection, with no restriction on the signal to be detected.

If $\sigma_0 > \sigma_1$
  Let $\sigma_2 = \sqrt{\sigma_0^2 - \sigma_1^2}$
  If $(m_1 - m_0)^2 + 2\sigma_2^2 \ln[(\sigma_0 P_1)/(\sigma_1 P_0)] > 0$
    Let $m_2 = \sqrt{(m_1 - m_0)^2 + 2\sigma_2^2 \ln[(\sigma_0 P_1)/(\sigma_1 P_0)]}$
    Let $Y_{T1} = (\sigma_0^2 m_1 - \sigma_1^2 m_0 - \sigma_0\sigma_1 m_2)/\sigma_2^2$
    Let $Y_{T2} = (\sigma_0^2 m_1 - \sigma_1^2 m_0 + \sigma_0\sigma_1 m_2)/\sigma_2^2$
    If $Y_{T1} < T(\mathbf{Y}) < Y_{T2}$ **decide** H_1 Else **decide** H_0 End If
    $P_{\mathrm{er}} = \frac{1}{2}\left[\mathrm{erf}\left(\frac{Y_{T2}-m_0}{\sqrt{2}\sigma_0}\right) - \mathrm{erf}\left(\frac{Y_{T1}-m_0}{\sqrt{2}\sigma_0}\right)\right]P_0 + \left[1 + \frac{1}{2}\mathrm{erf}\left(\frac{Y_{T1}-m_1}{\sqrt{2}\sigma_1}\right) - \frac{1}{2}\mathrm{erf}\left(\frac{Y_{T2}-m_1}{\sqrt{2}\sigma_1}\right)\right]P_1$
  Else
    decide H_0
    $P_{\mathrm{er}} = P_1$
  End If
Else If $\sigma_0 < \sigma_1$
  Let $\sigma_2 = \sqrt{\sigma_1^2 - \sigma_0^2}$
  If $(m_1 - m_0)^2 + 2\sigma_2^2 \ln[(\sigma_1 P_0)/(\sigma_0 P_1)] > 0$
    Let $m_2 = \sqrt{(m_1 - m_0)^2 + 2\sigma_2^2 \ln[(\sigma_1 P_0)/(\sigma_0 P_1)]}$
    Let $Y_{T1} = (\sigma_1^2 m_0 - \sigma_0^2 m_1 - \sigma_0\sigma_1 m_2)/\sigma_2^2$
    Let $Y_{T2} = (\sigma_1^2 m_0 - \sigma_0^2 m_1 + \sigma_0\sigma_1 m_2)/\sigma_2^2$
    If $Y_{T1} < T(\mathbf{Y}) < Y_{T2}$ **decide** H_0 Else **decide** H_1 End If
    $P_{\mathrm{er}} = \left[1 + \frac{1}{2}\mathrm{erf}\left(\frac{Y_{T1}-m_0}{\sqrt{2}\sigma_0}\right) - \frac{1}{2}\mathrm{erf}\left(\frac{Y_{T2}-m_0}{\sqrt{2}\sigma_0}\right)\right]P_0 + \frac{1}{2}\left[\mathrm{erf}\left(\frac{Y_{T2}-m_1}{\sqrt{2}\sigma_1}\right) - \mathrm{erf}\left(\frac{Y_{T1}-m_1}{\sqrt{2}\sigma_1}\right)\right]P_1$
  Else
    decide H_1
    $P_{\mathrm{er}} = P_0$
  End If
Else If $\sigma_0 = \sigma_1$
  Let $Y_T = \frac{m_0+m_1}{2} + \frac{\sigma_0^2}{m_1-m_0}\ln(P_0/P_1)$
  If $T(\mathbf{Y}) > Y_T$ **decide** H_1 Else **decide** H_0 End If
  $P_{\mathrm{er}} = \frac{1}{2}\left[1 + P_1\,\mathrm{erf}\left(\frac{Y_T-m_1}{\sqrt{2}\sigma_0}\right) - P_0\,\mathrm{erf}\left(\frac{Y_T-m_0}{\sqrt{2}\sigma_0}\right)\right]$
End If

Fig. 3. Detection algorithm to compute and assess the performance of the nonlinear detector which is the MAP test based on the statistic $T(\mathbf{Y})$. The algorithm takes as input the set of quantities $\{T(\mathbf{Y}),\ m_0 = E[T(\mathbf{Y})|\mathrm{H}_0],\ m_1 = E[T(\mathbf{Y})|\mathrm{H}_1],\ \sigma_0^2 = \mathrm{var}[T(\mathbf{Y})|\mathrm{H}_0],\ \sigma_1^2 = \mathrm{var}[T(\mathbf{Y})|\mathrm{H}_1]\}$ and gives as output the theoretical performance P_{er} and the result of the decision for a given numerical trial for the nonlinear detector of Fig. 1b.

4. Comparing performances of the linear and nonlinear detector

We now come to compare the probability of detection error P_{er} of the nonlinear detector of Fig. 1b (given in Fig. 3) and the linear detector of Fig. 1a (given in Eq. (5)) for various conditions concerning the input noise $\xi(t)$ and the type of signals to be detected.

We first consider the case where the input noise $\xi(t)$ is zero-mean Gaussian. Fig. 4 shows the evolution of the probability of error P_{er} of Fig. 3, as a function of the rms amplitude σ_η of the quantizer noises $\eta_i(t)$, for various sizes M of the array. In these conditions, where $\xi(t)$ is Gaussian, the linear detector represents the optimal detector (in terms of lowest probability of error P_{er}) based on the data set $\mathbf{x}$. Therefore, in Fig. 4, the nonlinear detector cannot produce a lower P_{er}. Nevertheless, the performance of the nonlinear detector comes close to that of the best detector. As demonstrated at the origin of Fig. 4, this is already the case when no noise is present in the array $\sigma_\eta = 0$ although requiring only a parsimonious 1-bit representation of each data sample x_i. This observation is consistent with the one given in [19]. The new

[2]We will discuss in the next section what is the order of magnitude required to have this large data set condition fulfilled.

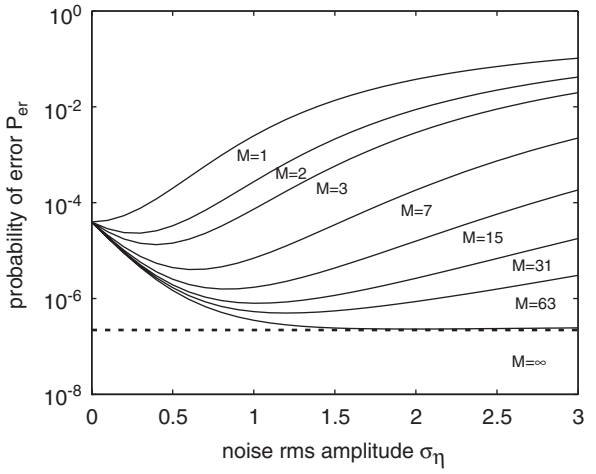

Fig. 4. Probability of detection error P_{er}, as a function of the rms amplitude σ_η of the uniform zero-mean white noises $\eta_i(t)$ purposely added to the quantizer input. The solid lines are the theoretical P_{er} of the nonlinear detector of Fig. 1b calculated from the algorithm in Fig. 3, for various size M of the array of two-state quantizer, when the input noise $\xi(t)$ is chosen Gaussian. The dashed line is the performance of the linear detector of Fig. 1a given in Eq. (4). The other parameters are $s(t) = A$ with $A/\sigma_\xi = 1$, $P_0 = 0.5$ and $N = 100$.

feature here is that it is possible to improve the performance of the nonlinear detector for a single two-state quantizer. This improvement is obtained by simply replicating the two-state quantizer and then by injecting a certain amount of independent noises in the array of quantizers. At $M>1$, application of the quantizer noises $\eta_i(t)$ allows the quantizers to respond differently. For the nonlinear detector, this translates into a possibility of minimizing P_{er} with a non-zero optimal amount of the quantizer noises. The benefit from noise is especially visible in Fig. 4, when the size of the array M increases. The explicit computation of the asymptotic behavior in large arrays is available from Eq. (15) by considering M tending to ∞. If the array size M tends to ∞, and if the optimal amount of noise is added in the array, the performance of the nonlinear detector asymptotically reaches the overall minimum probability of error P_{er} of the linear detector. This last statement, concerning the convergence of the nonlinear detector toward the linear detector, can be proved explicitly in the case of Fig. 4. As previously explained, when M tends to ∞, the array of noisy quantizers acts like a deterministic single device with input–output characteristic $g(x) = E[Y|x] = 1 - 2F_\eta(\theta - x)$ according to Eq. (12). In Fig. 4, the quantizer noises $\eta_i(t)$,

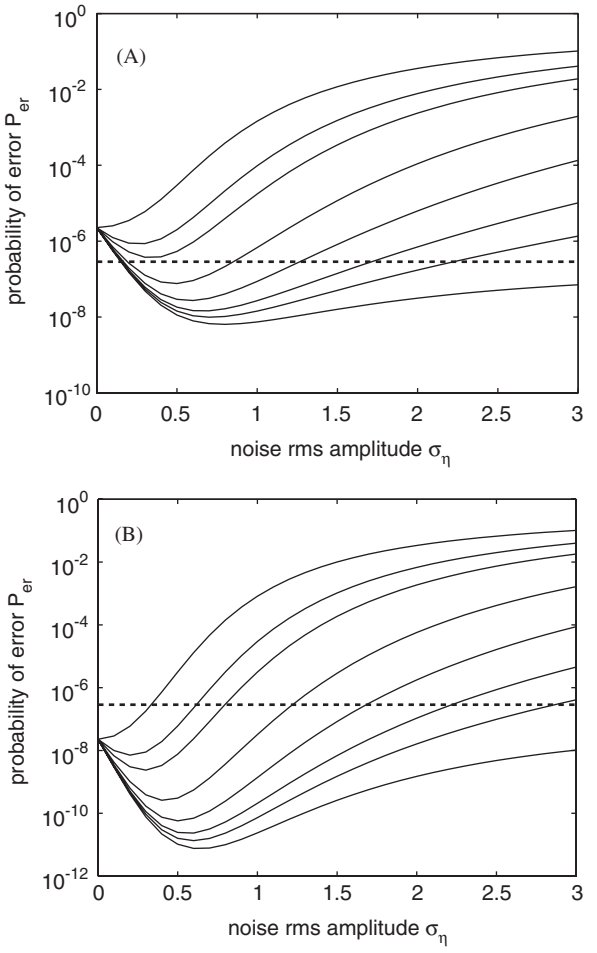

Fig. 5. Influence of the density $f_\xi(u)$ of the input noise $\xi(t)$. Panel A: same as Fig. 4 but the input noise $\xi(t)$ is zero-mean Laplacian, i.e. $\xi(t)$ is generalized Gaussian with exponent $\alpha = 1$. Panel B: same as panel A but the input noise $\xi(t)$ is a zero-mean mixture of Gaussian with parameters $\alpha = 0.8$ and $\beta = 4$. In both panels (A,B), the dashed lines stand for the performance of the linear detector given by Eq. (5).

chosen uniform, linearize the input–output characteristic $g(.)$ of the array.

When the input noise $\xi(t)$ is non-Gaussian, the linear detector is suboptimal and represents the best detection when basing the detection on $T(\mathbf{x})$ only. In this case, the nonlinear detector can produce lower P_{er} as shown in Fig. 5. This is the case when $\xi(t)$ is non-Gaussian and belongs to the generalized Gaussian noise family or the mixture of Gaussian noise family. The generalized Gaussian noise family is expressed as $f_\xi(u) = f_{gg}(u/\sigma_\xi)/\sigma_\xi$, using the standardized density

$$f_{gg}(u) = A\exp(-|bu|^\alpha), \tag{19}$$

where $b=[\Gamma(3/\alpha)/\Gamma(1/\alpha)]^{1/2}$, $A=(\alpha/2)[\Gamma(3/\alpha)]^{1/2}/[\Gamma(1/\alpha)]^{3/2}$ are parameterized by the positive exponent α. This family includes the Gaussian case ($\alpha=2$) but also enables leptokurtic noise densities whose tails are either heavier ($\alpha<2$) or lighter ($\alpha>2$) than that of the Gaussian noise. The mixture of Gaussian pdf is expressed as $f_\xi(u)=f_{\mathrm{mg}}(u/\sigma_\xi)/\sigma_\xi$, using the standardized density

$$f_{\mathrm{mg}}(u)=\frac{c}{\sqrt{2\pi}}\left[\alpha\exp\left(-\frac{c^2u^2}{2}\right)+\frac{1-\alpha}{\beta}\exp\left(-\frac{c^2u^2}{2\beta^2}\right)\right], \tag{20}$$

where $c=[\alpha+(1-\alpha)(\beta^2)]^{1/2}$; $\alpha\in[0,1]$ is the mixing parameter and $\beta>0$ is the ratio of the standard deviations of the individual contributions. All the pdf of the mixture of Gaussian noise family have Gaussian tails. This family of pdf's has practical implication since it is a subclass of Middleton's class which is widely used to model ocean acoustic noise [20]. As illustrated in Fig. 5, our analysis establishes that the superiority of the nonlinear detector over the linear detector especially occurs for various situations of non-Gaussian noises $\xi(t)$ having Gaussian or heavy tails.

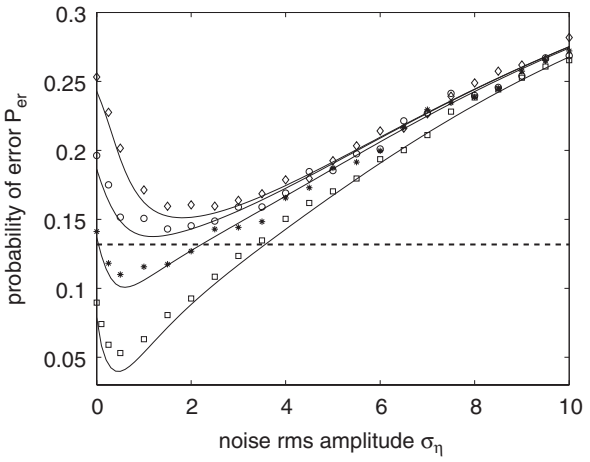

Fig. 6. Probability of detection error P_{er}, as a function of the rms amplitude σ_η of the Gaussian zero-mean white noise $\eta_i(t)$ purposely added to the quantizer input. The solid lines are the theoretical P_{er} of the nonlinear detector of Fig. 1b calculated from the algorithm in Fig. 3, with a quantizer array of fixed size $M=63$, for various probability densities of the input noise $\xi(t)$ according to Eq. (19). The discrete data points are the corresponding numerical estimations of P_{er} over 10^4 trials with: ($\diamond$) $\alpha=\infty$ (ξ uniform), ($\circ$) $\alpha=2$ (ξ Gaussian), ($*$) $\alpha=1$ (ξ Laplacian), ($\square$) $\alpha=\frac{1}{2}$. The dashed line is the performance of the linear detector scheme based on the linear statistic $T(\mathbf{x})$ of Eq. (4) given by the same algorithm in Fig. 3. The other parameters are $s(t)=A\cos(2\pi t/T_s)$, $A/\sigma_\xi=1$, $P_0=0.5$, $\tau=T_s/10$ and $N=10$.

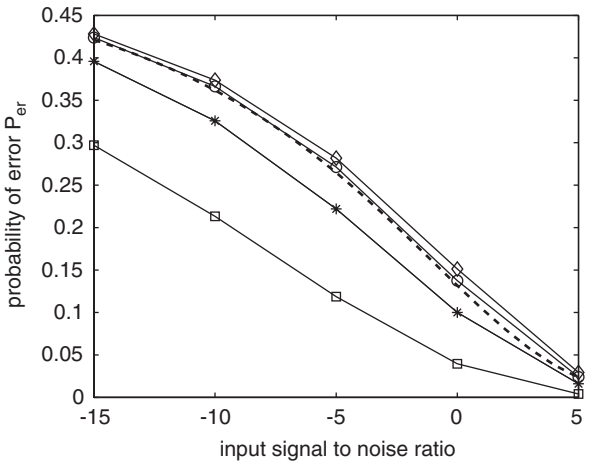

Fig. 7. Best performance of the nonlinear detector error as a function of the input signal-to-noise ratio in dB. For each discrete point the rms amplitude σ_η of the Gaussian zero-mean white noise $\eta_i(t)$ purposely added to the quantizer input is fixed in order to minimize the probability of error. Same conditions as in Fig. 6 except the solid lines which are just guides for the eye. In the context of Fig. 6, the input signal-to-noise ratio in dB is $10\log_{10}((A^2/2)/\sigma_\xi^2)$.

Fig. 6 offers a validation of the nonlinear detection algorithm of Fig. 3 through the numerical evaluation of P_{er}. The results of Fig. 3 are obtained on data sets of size $N=10$. They show that the algorithm of Fig. 3 and the associated expressions of P_{er} although valid in principle in the large N limit, also constitute a very good approximation for small N. Therefore, the superiority observed for the nonlinear detector over the linear detector (due to the presence of the nonlinear array used as preprocessor) and the performance gain brought by the injection of independent noises in the array are robustly preserved for small data sets N. Fig. 7 demonstrates that this superiority of the nonlinear detector over the linear detector is available over a large range of input signal-to-noise ratio.

5. Enlarging to a Neyman–Pearson detection strategy

In this section, we show that the usefulness of the nonlinear array of Fig. 2, when the input noise $\xi(t)$ is non-Gaussian, can easily be extended to another detection strategy. Until now, we have compared the detection performance of the linear detector and the nonlinear detector of Fig. 1 assessed by the

probability of error (expected as small as possible). This Bayesian detection strategy requires that probabilities (P_0, $P_1 = 1 - P_0$) of both hypotheses (respectively, H_0, H_1) of Eq. (2) are known. This assumption, typically valid in the domain of telecommunication, is not possible in other applications such as sonar or radar [2]. When P_0 and P_1 are unknown, if the decision between (hypothesis H_1) and (hypothesis H_0) is directly based on the linear signal–noise mixture, the observable data set $\mathbf{x}$, a strategy to implement an optimal detection is to seek to maximize the probability of detection

$$P_D = \int_{\mathscr{R}_1} p(\mathbf{x}|H_1)\,d\mathbf{x}, \tag{21}$$

while keeping the probability of false alarm

$$P_F = \int_{\mathscr{R}_1} p(\mathbf{x}|H_0)\,d\mathbf{x} \tag{22}$$

no larger than a prescribed level $P_{F,sup}$. This constrained maximization is achieved by the optimal Neyman–Pearson detector, which also implements a likelihood-ratio test. When the input noise $\xi(t)$ is Gaussian the best detector in the Neyman–Pearson sense takes a form very similar to the linear detector described in Fig. 1a [2]: a correlation receiver which computes the statistic $T(\mathbf{x}) = \sum_{j=0}^{N-1} x(t_j)s(t_j)$ is followed by the Neyman–Pearson likelihood-ratio test based on this statistic $T(\mathbf{x})$,

$$L(T(\mathbf{x})) \underset{H_0}{\overset{H_1}{\gtrless}} \mu(P_{F,sup}), \tag{23}$$

with a threshold $\mu(P_{F,sup})$, a function of $P_{F,sup}$, which is found from Eq. (22) by imposing $P_F \leqslant P_{F,sup}$. The probability of detection of this Neyman–Pearson linear detector is given by

$$P_D = \mathrm{erfc}\left(\mathrm{erfc}^{-1}(P_{F,sup})\frac{\sigma_0}{\sigma_1} - \frac{m_1 - m_0}{\sigma_0}\right) \tag{24}$$

with, for $k \in \{0,1\}$, means $m_k = E[T(\mathbf{x})|H_k]$, variance $\sigma_k^2 = \mathrm{var}[T(\mathbf{x})|H_k]$ and $\mathrm{erfc}(u) = \int_u^{+\infty}(1/\sqrt{2\pi})\exp(-v^2/2)\,dv$. When the input noise $\xi(t)$ is non-Gaussian, the optimal detector in the Neyman–Pearson, in general, is difficult to design. The same nonlinear array of Fig. 2 can be used again as preprocessor to design a simple suboptimal nonlinear detector capable of outperforming the Neyman–Pearson linear detector when the input noise $\xi(t)$ is non-Gaussian. Therefore, this Neyman–Pearson nonlinear detector first applies the observable data set $\mathbf{x} = (x(t_1), \ldots, x(t_N))$ at the input of the nonlinear array of Fig. 2 which produces a vector $\mathbf{Y} = (Y(t_1), \ldots, Y(t_N))$. The Neyman–Pearson nonlinear detector is then composed of a correlation receiver which computes the statistic $T(\mathbf{Y}) = \sum_{j=0}^{N-1} Y(t_j)s(t_j)$ followed by the likelihood-ratio test based on this statistic $T(\mathbf{Y})$,

$$L(T(\mathbf{Y})) \underset{H_0}{\overset{H_1}{\gtrless}} \mu(P_{F,sup}). \tag{25}$$

The performance of the Neyman–Pearson nonlinear detector of Eq. (23) is given by Eq. (24) with, for $k \in \{0,1\}$, $m_k = E[T(\mathbf{Y})|H_k]$, variance $\sigma_k^2 = \mathrm{var}[T(\mathbf{Y})|H_k]$, which have been given in Section 3. Fig. 8 shows that the Neyman–Pearson nonlinear detector can produce larger P_D than the one produced by the Neyman–Pearson linear detector when the noise is non-Gaussian. This observation, consistent with the result presented in Figs. 5 and 6 for another detection strategy, enlarges the usefulness of the nonlinear array of Fig. 2 as preprocessor for detection purposes.

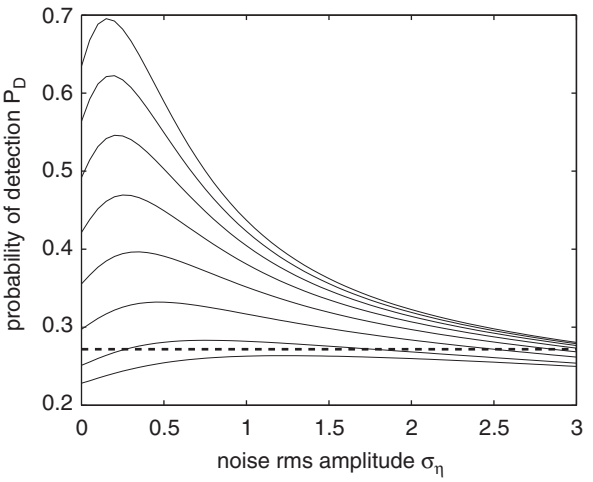

Fig. 8. Probability of correct detection P_D for a fixed probability of false alarm $P_{F,sup} = 0.1$, as a function of the rms amplitude σ_η of the Gaussian zero-mean white noise $\eta_i(t)$ purposely added to the quantizer input. The solid lines are the theoretical P_D of the Neyman–Pearson nonlinear detector of Eq. (25) calculated from Eq. (24), with a quantizer array of fixed size $M = 63$, for various probability densities of the input noise $\xi(t)$ according to Eq. (20). From up to bottom, the input noise $\xi(t)$ is a mixture of Gaussian with parameters $\alpha = 0.8$ and $\beta = 8, 7, 6, 5, 4, 3, 2, 1$. The dashed line is the performance of the Neyman–Pearson linear detector of Eq. (25) given by Eq. (24). The other parameters are $s(t) = A\exp(-vt)\cos(2\pi t/T_s)$, $A/\sigma_\xi = 1$, $v = 100/T_s$, $\tau = T_s/20$ and $N = 100$.

6. Discussion

We have studied the usefulness of a specific nonlinear preprocessor, a parallel array of two-state quantizers, to design simple suboptimal detectors in non-Gaussian noise. To do so, we have considered a standard two hypotheses detection problem and we have assessed the performance of two kinds of detectors:

(i) Standard linear detectors, optimal in Gaussian noise, composed of a correlation receiver followed by a binary test.
(ii) Nonlinear detectors, composed of the nonlinear preprocessor under study followed by a structure identical to the one of the linear detectors.

The performance of these linear and nonlinear detectors have been compared in a Bayesian and in a Neyman–Pearson detection strategy when the signal to be detected and the native non-Gaussian noise are known a priori. This comparison is meaningful since the linear detectors are often used even when the noise is a priori known to be non-Gaussian. This suboptimal choice is specially made for fast real-time hard processing, to maintain a simple test statistic on which to base the detection. The nonlinear detector considered here is almost as fast to compute as the linear detector. In addition of being compatible with a fast real-time hard implementation, we have shown that this nonlinear detector can achieve better performance compared to the linear detector for various non-Gaussian noise of practical interest. As illustrated in this article, this occurs for both Bayesian and Neyman–Pearson detection strategy with a large range of input signal $s(t)$ amplitude with various types including constant signals (in Figs. 4 and 5), periodic signals (in Fig. 6) and aperiodic signals (in Fig. 8).

These results have been obtained with a non-standard configuration of the parallel array quantizers. Instead of adopting a classical distributed-threshold configuration, we have used a simpler common-threshold configuration in which some noise have purposely been injected in order to shape the input–output characteristic of the array seen as a single device. The resulting input–output characteristic of the array depends on the choice of the injected noises and quantizer characteristics. In this article, we have chosen to study an array of two-state quantizers associated with noises in the array that were uniform or Gaussian. Many other associations could be investigated with variations concerning the type of noises injected in the array or the characteristic of the quantizers. It is remarkable to note that the simple associations tested in this study can be useful to design suboptimal detectors for the variety of non-Gaussian noise pdf that we have explored here. Such simple associations of standard noises and existing electronic devices which can easily be replicated, at a micro- or nano-scale, to constitute large arrays, could also exist for other detection problem in non-Gaussian noises of practical interest (like speckle noise in coherent imaging). These research could benefit from the theoretical framework of this study since it allows to consider any kind of static nonlinearity. Another possible interesting extension would be to draw the design of adaptive procedures, which would extend those introduced for conventional stochastic resonance [21] and which would let the array automatically increase the array noises above zero until an optimal efficacy is reached.

At a general level, this report contributes to extend our understanding of noise enhanced signal processing. The idea that an addition of a certain controlled amount of noise can be useful in the processing of information carrying signals by static quantizers is not new in itself. All occurrences of this phenomenon in static quantizers are often thought to illustrate the dithering effect [22]. In this well-known dithering effect, a noise induces threshold crossing and linearizes on average the quantizer characteristic. This is clearly not the case here since when the input noise has a non-Gaussian pdf, averaging the individual independent response of the two-state quantizers leads to a collective detection performance that outperforms the linear detector applied to the original analog data. This proves that the noise-enhanced detection performance reported here cannot be interpreted as a noise-induced linearization of a nonlinear system. Many counter-intuitive contributions of noise in nonlinear signal processing may still be uncovered and ought to be analyzed in detail.

References

[1] D.L. Duttweiler, T. Kailath, RKHS approach to detection and estimation problems—part IV: non-Gaussian detection, IEEE Trans. Inform. Theory 19 (1973) 19–28.
[2] S. Kay, Fundamentals of Statistical Signal Processing: Detection Theory, Prentice-Hall, Englewood Cliffs, NJ, 1998.

[3] N.H. Lu, B.A. Einstein, Detection of weak signals in non-Gaussian noise, IEEE Trans. Inform. Theory IT-27 (1981) 755–771.
[4] S. Kassam, Optimum quantization for signal detection, IEEE Trans. Comm. 25 (1977) 479–484.
[5] H.V. Poor, J.B. Thomas, Applications of Ali–Silvey distance measures in the design of generalized quantizers for binary decision systems, IEEE Trans. Comm. 25 (1977) 893–900.
[6] B. Aazhang, H.V. Poor, On optimum and nearly optimum data quantization for signal detection, IEEE Trans. Comm. 32 (1984) 745–751.
[7] B. Picinbono, P. Duvaut, Optimum quantization for detection, IEEE Trans. Comm. 36 (1988) 1254–1258.
[8] C. Duchene, P.-O. Amblard, S. Zozor, Quantizer-based suboptimal detectors: noise-enhanced performance and robustness, International Symposium on Fluctuations and Noise (FN'05), Proceedings of the SPIE, vol. 5847, Austin, TX, USA, 23–26 May 2005, pp. 100–110.
[9] N.G. Stocks, Suprathreshold stochastic resonance in multilevel threshold systems, Phys. Rev. Lett. 84 (2000) 2310–2313.
[10] N.G. Stocks, Information transmission in parallel threshold arrays: suprathreshold stochastic resonance, Phys. Rev. E 63 (2001) 041114,1–9.
[11] M.D. McDonnell, D. Abbott, C.E.M. Pearce, A characterization of suprathreshold stochastic resonance in an array of comparators by correlation coefficient, Fluctuation Noise Lett. 2 (2002) L205–L220.
[12] D. Rousseau, F. Duan, F. Chapeau-Blondeau, Suprathreshold stochastic resonance and noise-enhanced Fisher information in arrays of threshold devices, Phys. Rev. E 68 (2003) 031107,1–10.
[13] D. Rousseau, F. Chapeau-Blondeau, Suprathreshold stochastic resonance and signal-to-noise ratio improvement in arrays of comparators, Phys. Lett. A 321 (2004) 280–290.
[14] D. Rousseau, F. Chapeau-Blondeau, Constructive role of noise in signal detection from parallel arrays of quantizers, Signal Processing 85 (2005) 571–580.
[15] X. Godivier, F. Chapeau-Blondeau, Noise-assisted signal transmission in a nonlinear electronic comparator: experiment and theory, Signal Processing 56 (1997) 293–303.
[16] L. Gammaitoni, P. Hänggi, P. Jung, F. Marchesoni, Stochastic resonance, Rev. Mod. Phys. 70 (1998) 223–287.
[17] E. Pantazelou, F. Moss, D. Chialvo, Noise sampled signal transmission in an array of Schmitt triggers, in: P.H. Handel, A.L. Chung (Eds.), Noise in Physical Systems and $1/f$ Fluctuations, AIP Conference Proceedings, vol. 285, New York, 1993, pp. 549–552.
[18] J.J. Collins, C.C. Chow, T.T. Imhoff, Stochastic resonance without tuning, Nature 376 (1995) 236–238.
[19] F. Chapeau-Blondeau, Nonlinear test statistic to improve signal detection in non-Gaussian noise, IEEE Signal Process. Lett. 7 (2000) 205–207.
[20] F.W. Machell, C.S. Penrod, G.E. Ellis, Statistical characteristics of ocean acoustic noise process, in: E.J. Wegman, S.C. Schwartz, J.B. Thomas (Eds.), Topics in Non-Gaussian Signal Processing, Springer, Berlin, 1989, pp. 29–57.
[21] B. Kosko, S. Mitaim, Robust stochastic resonance: signal detection and adaptation in impulsive noise, Phys. Rev. E 64 (2001) 051110,1–11.
[22] L. Gammaitoni, Stochastic resonance and the dithering effect in threshold physical systems, Phys. Rev. E 52 (1995) 4691–4698.